FIRST RESULTS FROM THE SPI IMAGING TEST SETUP

C. B. Wunderer[1], R. Diehl[1], R. Georgii[1], A. von Kienlin[1], G. Lichti[1], A. W. Strong[1], V. Schönfelder[1], G. Vedrenne[2], F. Sanchez[3], and P. Connell[4]

[1]Max-Planck-Institut für extraterrestrische Physik, 85748 Garching, Germany
[2]CESR, Toulouse, France
[3]Universidad de Valencia, Valencia, Spain
[4]University Birmingham, Birmingham, United Kingdom

ABSTRACT

The SPI Imaging Test Setup (SPITS) was built for experimental verification of the imaging properties of SPI. SPITS provides the possibility to validate simulations - needed for SPI image reconstruction - with laboratory measurements. SPITS consists of a coded mask and two Germanium detectors; no anti-coincidence system is used. The mask has the same Tungsten-alloy HURA coding as SPI. The two hexagonal Ge-detectors are housed in a common Al end cap. They can be moved to cover the 19 SPI Ge-detector positions. Mask and Germanium detectors are made of SPI-FM materials. The imaging properties of SPITS are being measured with radioactive sources 9 m from the detector plane. We obtain an angular resolution of about 2^o at 1.8 MeV and a point-source location capability of SPITS of 15' at 1.2 MeV, both for strong sources.

Key words: INTEGRAL; SPI; coded mask imaging.

1. INTRODUCTION

All of INTEGRAL's instruments except the optical monitor use Tungsten-alloy coded masks to obtain directional information. Although coded masks are well known in the X-ray domain (e.g. Badiali (1985) and references therein), INTEGRAL's instruments will be the first spaceborne detector systems using coded masks up to 10 MeV. INTEGRAL is a follow-up of the SIGMA experiment (Paul, 1991), with improved sensitivity and an increased energy range. In SPI, for the first time, high-purity Germanium (HPGe) detectors are combined with a coded aperture to perform astrophysical observations on a satellite platform. The tungsten-alloy mask elements are 30 mm thick, enough to absorb gamma rays up to several MeV. Each of the 19 hexagonal Ge crystals has a front area of 27 cm^2 and is 7 cm long.

Studies of the imaging capabilities of SPI were performed using GEANT and other simulation tools (Skinner, 1997; Connell, 1999; Strong, 1999). The SPI Imaging Test Setup (SPITS) was built to complement theoretical studies of SPI imaging performance and to provide the chance to test SPI data-analysis methods on experimental data long before launch. SPITS results will complement findings from the SPI calibrations which will take place in 2001.

2. THE SPI IMAGING TEST SETUP

SPITS' coded mask is equivalent to the SPI mask. Built on the basis of the SPI mask development model, it consists of SPI materials and is coded in the SPI "hexagonal uniformly redundant array" (HURA) pattern. The array of 19 HPGe detectors that makes up the camera of SPI was replaced by only two detectors; they can be moved with an XY-table to all 19 SPI Ge-detector positions. The individual Ge crystals in their Al capsules are from the SPI detector manufacturing line and cooled with liquid nitrogen. The SPI Be cryostat and cold plate were replaced by (thinner) Al parts. A drawing of SPITS is shown in Figure 1, a more detailed description is given in Wunderer (2001). The SPI telescope is equipped with a BGO anticoincidence shield to allow discrimination against particles entering the telescope from the sides. There is also a 5 mm plastic scintillator anticoincidence shield (PSAC) between mask and Ge detectors. Since background radiation on the ground is at a much lower level, neither is required for SPITS. However, to account for the PSAC's influence on the mask transmissivity, a plexiglass sheet of equivalent thickness was mounted.

3. MEASUREMENTS

For the measurements described here, we used ^{60}Co (1173 keV, 1332 keV) and ^{88}Y (898 keV, 1836 keV)

point sources (diameter of active volume $\approx$ 1 mm). They were placed in a holder 9 m from the SPITS detector plane, with positioning accurate to less than 0.5 arcmin. The ^{60}Co-source was moved horizontally away from the SPITS instrument axis, initially in steps as small as 2.5'. At each source position, an image was measured with 3600 s exposure time for each Ge-detector position. The ^{88}Y-source was put at 0^o, 0.5^o, ... 4.5^o from the instrument axis. Data from two such measurements were added to form a composite dataset of two sources which are separated by 0.5^o to 4.5^o. We also measured the photopeak efficiency of the Ge-detectors. With this information, we can determine how accurately present SPI imaging analysis software is able to reconstruct the intensity of the calibration sources used.

4. SPITS IMAGE DECONVOLUTION

For SPI image analysis, two methods are foreseen: (1) *spiskymax* (Strong, 1995), a program based on the maximum-entropy method, and (2) *spiros* (Connell, 2000), an algorithm that iteratively removes point sources from the image as it determines their location and strength using correlation matrices. In this work, we apply only the maximum-entropy method. SPI image deconvolution algorithms use instrument response functions (IRFs) that reflect the response of all 19 detectors to a source of a given energy at any point in the sky. Since this response is different for sources at infinity and at a finite distance - the shadow projection of the mask onto the detector plane is not the same - we use IRFs that fit the SPITS source-detector geometry. These IRFs were calculated using a ray-tracing algorithm (SPI IRFs will be built using GEANT).

5. ANGULAR RESOLUTION AND POINT SOURCE LOCATION ACCURACY

To determine SPITS' ability to accurately locate a strong ^{60}Co source, we measured image data with this source positioned at 0', 2.5', 5', 10', 20', ... 60' from the instrument axis. In order to estimate SPITS' source-location capability independent of image reconstruction, we calculate the normalized χ^2 between two such sets of image raw data. The farther the source positions are apart, the larger the difference between the datasets should be. If more than one pair of datasets has the required angular distance between source positions, we show up to three results (Table 1) to demonstrate the range of values for the 1173 keV and 1332 keV lines of ^{60}Co. For comparison, normalized χ^2 values are also shown for the 1461 keV line from natural ^{40}K, an isotope which is roughly isotropic in the laboratory environment. Assuming that a normalized χ^2 of 15 signifies that data is sufficiently distinct, determination of source locations to 7.5 or 10 arcmin seems feasible for single strong sources in a virtually background-free environment.

Table 1. Normalized χ^2 from comparison of two datasets taken with a single strong ^{60}Co source at different positions; 1460 keV line from natural ^{40}K added for comparison

angular distance [arcmin]	Normalized χ^2 from binned data 1173 keV	1332 keV	1461 keV
2.5	5.16	3.22	2.38
2.5	3.17	3.62	1.22
5.0	7.74	8.87	2.31
5.0	8.24	6.03	1.39
5.0	5.87	9.03	0.71
7.5	17.84	16.12	1.15
10.0	28.15	26.61	1.88
10.0	29.81	23.50	1.39
15.0	63.64	49.52	1.07
20.0	92.67	84.25	1.06

Next, we deconvolved the image for each source position using *spiskymax*. Figure 2 shows a composite image of the results. In an attempt to quantify the deviation of the image source position from the true source position, we fit a two-dimensional gaussian to each image and calculate the distance from the peak of the gaussian to the true source position. This deviation was less than 15' for the sources at 0' to 40'. The width (σ) of the gaussian was between 10' and 20'. For 50' and 60', the maximum of the reconstructed image is too close to the border of the image for the fit to converge properly. Judging from this, for single strong sources close to the instrument axis a location capability of about 20 arcmin seems feasible with SPI and *spiskymax*. A second goal of SPITS is to determine the angular resolution of such an instrument, i.e. the capability to separate and correctly locate two close sources in a single image. We used the ^{88}Y data in the 1836 keV line for this task. As mentioned before, we added data from two measurements to obtain a dataset with two ^{88}Y sources. We tested several combinations of source positions with angular distances between 1.5^o and 2.5^o. Figures 3, 4, and 5 show three cases. Note how for sources that are too close to be separated properly the reconstructed image shows a source between the two true source positions (denoted by Xs). A more detailed description of these images is given in Wunderer (2001).

At 1836 keV, we superimposed masurements from a single 3.7 MBq ^{88}Y source. ^{88}Y has a half-life of only 107 days. Since the individual measurements were taken several days apart, the two sources in the images have somewhat different intensities. For the composite image in Figure 5 (2.5^o separation), this corresponds to 0.255$\pm$0.008

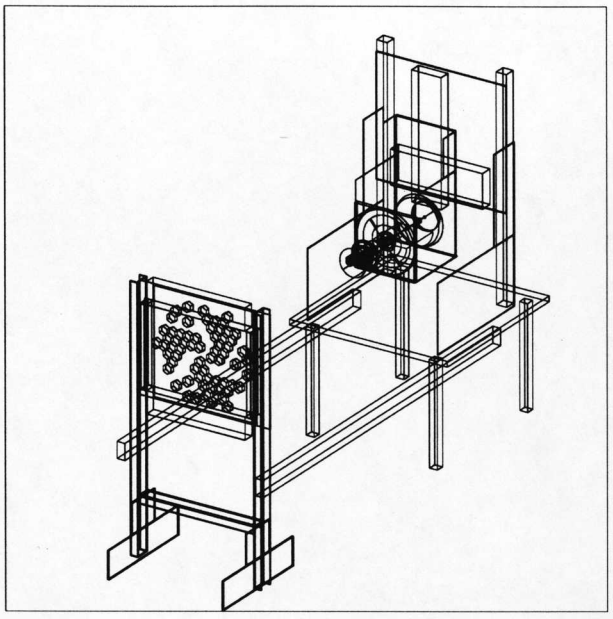

Figure 1. Schematic drawing of the SPI Imaging Test Setup.

photons/(cm^2 s sr) for source 1 at (0.5°, 0.87°) and 0.222±0.007 ph/(cm^2 s sr) for source 2 at (1.75°, 3.03°). (The uncertainty stems from the calibration of the ^{88}Y source activity.) The *spiskymax* algorithm finds these sources (intensity integrated over a circle with 0.5° radius and compared with a 1.0°-radius circle for background) with 6.3 σ and 5.1 σ significance, respectively. We obtain fluxes of 0.22±0.05 ph/(cm^2 s sr) for source 1 and 0.17±0.05 ph/(cm^2 s sr) for source 2. Within error bars, this is in agreement with the fluxes from the calibration source given above.

Table 2. Results from the reconstruction in the 1836 keV line of two ^{88}Y point sources, 2.5° apart, with background added to the data.

	fit	Bckgnd 10^3cts/det	Bckgnd 10^5cts/det
signal/bckgnd		2.65	0.0265
σ(0.5°, 0.9°)	7.9	4.5	2.8
σ(1.8°, 3.0°)	4.2	3.8	1.7
true flux at (0.5°, 0.87°): 0.255±0.008 ph/(cm^{2}s sr)			
skymax flux [ph/(cm^{2}s sr)]	0.21±0.04	0.21±0.06	0.17±0.07
true flux at (1.75°, 3.03°): 0.222±0.007 ph/(cm^{2}s sr)			
skymax flux [ph/(cm^{2}s sr)]	0.18±0.05	0.18±0.06	0.11±0.07

Above, we used virtually background-free data for our analysis. Since the measurements were performed in a laboratory environment, background levels were low. Furthermore, individual lines in the

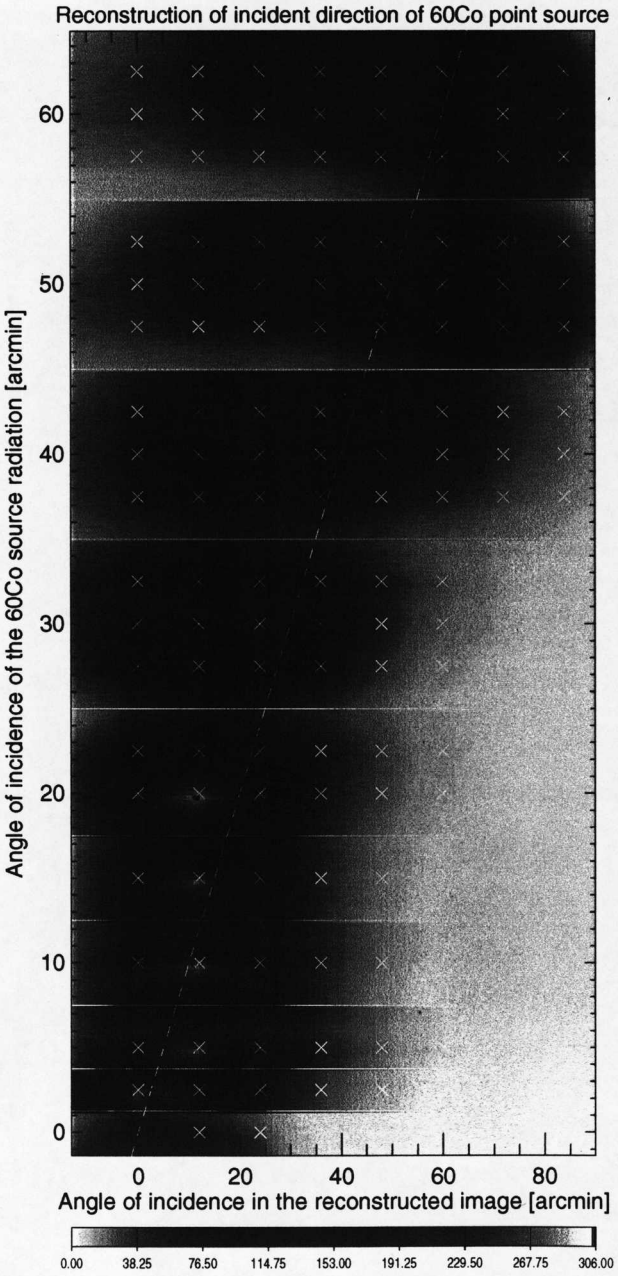

Figure 2. Composite of the reconstructed images of a ^{60}Co source at 0 to 60 arcmin from the instrument axis, source at 9 m. Reconstruction in the 1173 keV line performed using spiskymax. Grey Xs along the white dashed line mark true source positions, white Xs mark the gridpoints of the IRF.

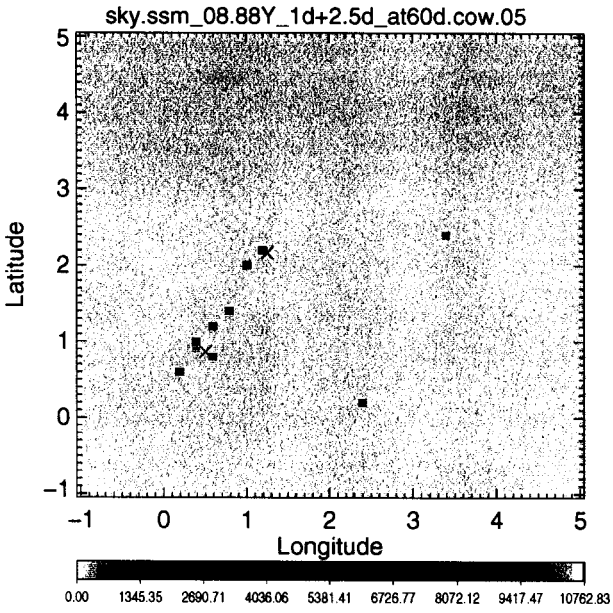

Figure 3. Reconstruction in the 1836 keV line of two ^{88}Y point sources at (0.5°, 0.87°) and (1.25°, 2.16°), 1.5° apart.

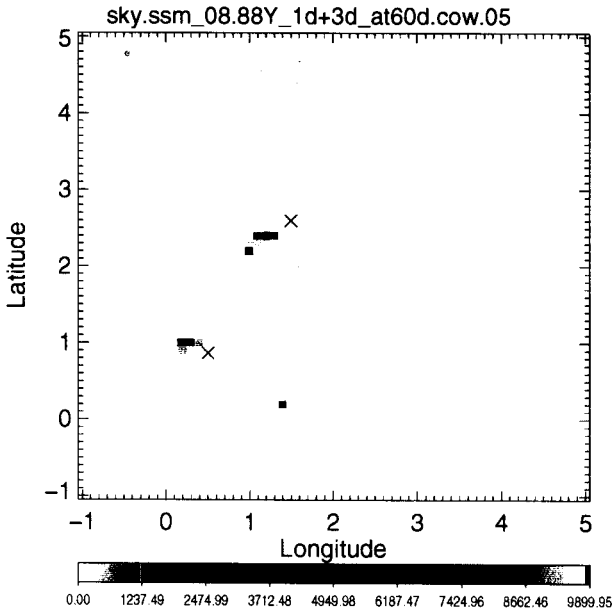

Figure 4. Reconstruction in the 1836 keV line of two ^{88}Y point sources at (0.5°, 0.87°) and (1.5°, 2.60°), 2.0° apart.

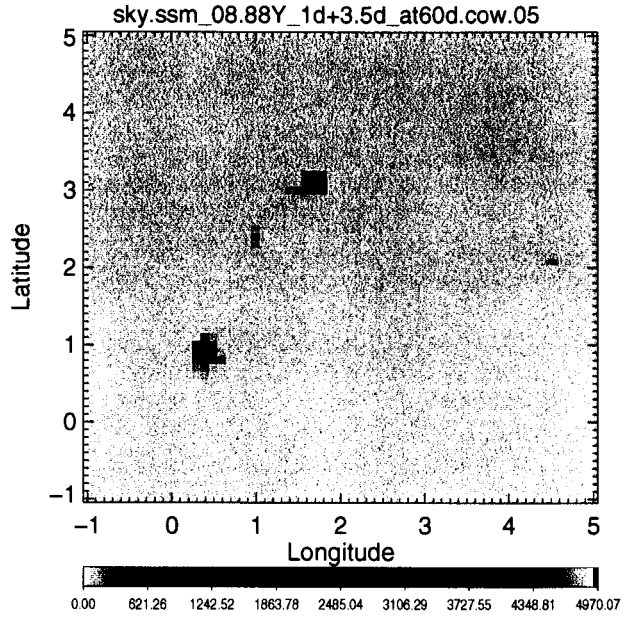

Figure 5. Reconstruction in the 1836 keV line of two ^{88}Y point sources at (0.5°, 0.87°) and (1.75°, 3.03°), 2.5° apart.

spectra were fitted and only the resulting peak areas fed to *spiskymax* for analysis. Here, we took the measurement shown in Figure 5 (two ^{88}Y sources) and compared results for the 1836 keV line obtained by (1) using the fitted data (Figure 5), (2) using all counts in an energy bin $\pm 3\sigma$ wide around the line energy and adding background to the data (poisson-distributed around 10^3 counts per detector), and (3) again using binned data and adding poisson-distributed background at the level of 10^5 counts per detector. The reconstructed images for cases (2) and (3) are shown in Figures 6 and 7, respectively. The images show $12° \times 12°$ of the 'sky', a larger section than Figures 3 to 5, to show artifacts that increase with increasing background levels. Table 2 summarizes the results; flux values are determined from an 1° radius around the true source position.

6. SUMMARY AND PLANS FOR THE FUTURE

We have demonstrated that SPITS, together with the *spiskymax* algorithm, can separate and correctly locate and determine the intensity of two point sources (2° or more apart) in one image. At 1836 keV, sources at a signal-to-noise level of 2.7 (0.027) are reconstructed with a significance of $\sim 4\ \sigma$ ($\sim 2\ \sigma$). χ^2-comparisons suggest that point-source location to $\sim$ 10' should be feasible while current *spiskymax* results are accurate to 15' for single strong sources at $\sim$ 1 MeV. Next steps with SPITS include determining point-source-location and angular resolution as function of energy. Furthermore, we will use *spiros* and compare its results with those from *spiskymax*.

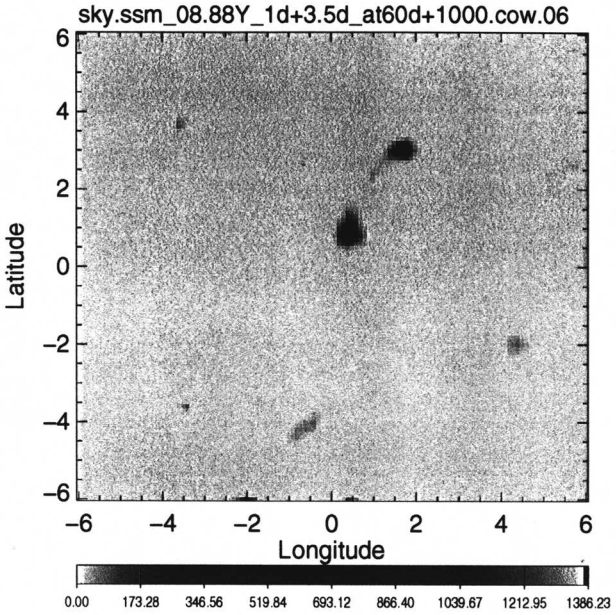

Figure 6. As Figure 5, but poisson-distributed background (10^3 counts/detector) added to the data.

REFERENCES

Badiali M., et al., 1985, A&A 151,259

Connell P., 1999, Proc. 3rd INTEGRAL Workshop 2, 397

Connell P., 2000, these proceedings

Paul J., et al., 1991, Adv. Space Res. 11 No.8,289

Skinner G. K., et al., 1997, Proc. 4th COMPTON Symposium 2, 1544

Strong A. W., 1995, Exp. Astronomy 6, 97

Strong A. W., 1999, Proc. 3rd INTEGRAL Workshop 2, 221

Wunderer C. B., et al., 2001, Trans. Nucl. Sci. Special Issue: Proc. IEEE Nuclear Science Symposium 2000, submitted

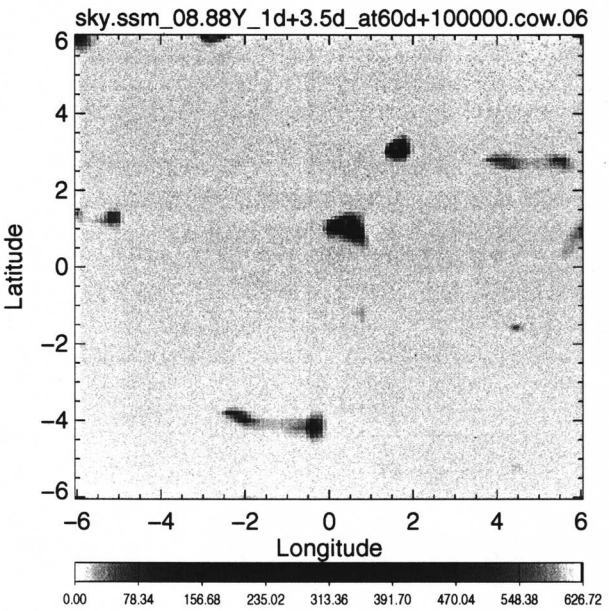

Figure 7. As Figure 5, but poisson-distributed background (10^5 counts/detector) added to the data.